

Flow resistance of partially flexible vegetation: A full-scale study with natural plants

Enrico Antonio Chiaradia, Claudio Gandolfi, Gian Battista Bischetti

Department of Agricultural and Environmental Sciences, Università degli Studi di Milano, Italy

Abstract

Riparian vegetation plays a crucial role in riverine ecosystems, providing many types of benefits to nature and humanity. However, a high vegetation density can reduce the conveyance capacity of a watercourse, particularly in the case of shrubs, which are very common within riverbeds and widely used in river and channel restoration works. In this paper, we study the influence of three species of shrubs (white and goat willows and black alder) on the hydraulic resistance factor of a real-scale channel under controlled flow conditions. A system for the anchorage of shrubs to the channel bed allowed us to carry out repeated experiments with the three plant species and with varying plant densities and flow rates. The experimental results provided a range of values for the additional contribution of the vegetation to the hydraulic resistance factor from 0.004 to 0.071 $\text{m}^{-1/3}\text{s}$, in terms of Manning's coefficient. This variability is related to the vegetation setup (plant species and density) but also to the increasingly hydrodynamic configuration assumed by plants at higher flow velocities and submergence ratios. We found that these factors can be summarised quite effectively by the product of elasticity (E), plant density (M), and plant area index (PAI). At small (E·M·PAI) values ($<10^8$) the

resistance coefficient is less than 0.01, while it increases of up to one order of magnitude when (E·M·PAI) exceeds 10^{10} . Furthermore, our results show a distinct two-stage trend of the value of the additional contribution to the n coefficient of a given vegetation setup at varying velocities and submergence levels, with values decreasing when a threshold of velocity and submergence ratio is exceeded. The position of this threshold point appears to be related to the geometrical and mechanical characteristics of the plants. Although our experiments do not provide enough data to identify a functional relationship between n and specific characteristics of the plants and of the flow, they show that the effect of shrubs on hydraulic resistance is highly variable with the flow conditions and that the conveyance capacity may be significantly larger than expected.

Introduction

Riparian vegetation plays a crucial role in riverine ecosystems, providing many benefits to nature and humanity (Bennet and Simon, 2004). Plants on riverbanks and floodplains, in fact, provide habitats and food resources for wildlife, improve geomorphologic stability and enhance aesthetic and recreational value (Pusey and Arthington, 2003; Merritt *et al.*, 2010). As a consequence, conservation and improvement of native riparian plants are frequently recommended by environmental agencies for river management and bank protection (*e.g.*, FISRWG, 1998), both by planting and by adopting soil bioengineering techniques. At the same time, however, it is equally widely recognised that riverine vegetation, especially shrubs and bushes, can reduce the conveyance capacity of a stream due to the increased hydraulic resistance and of the reduction of hydraulic sections (*e.g.*, Chow, 1959 p. 102).

In recent years, an increasing number of studies have been carried out to investigate the relationship between different types of vegetation and flow characteristics. Some of these studies have addressed fully flexible and fully submerged vegetation, such as grass and macrophytes (Temple, 1999; Yen, 2002; Carollo *et al.*, 2005; Kirkby *et al.*, 2005; Bal *et al.*, 2011; Nepf, 2012; Li *et al.*, 2014; Bebina Devi and Kumar, 2016; Errico *et al.*, 2018). The results that were obtained are robust, but their field of application is quite restricted (mainly grassed waterways and narrow streams). When shrubs and small riparian trees are concerned, as for example in many stream restoration works or in maintaining riparian vegetation on stream banks, their applicability is very limited.

Other studies focused on rigid non-submerged vegetation, typically trees (Ming and Shen, 1973; Arcement and Schneider, 1987; Yen, 2002; Järvelä, 2004; Kothyari *et al.*, 2009), providing a sound framework to consider its effect on flood propagation over floodplains, but they are of little use when semi-natural, mixed riverbank vegetation is at present.

Fewer studies have considered non-rigid and non-submerged

Correspondence: Enrico Antonio Chiaradia, Department of Agricultural and Environmental Sciences, Università degli Studi di Milano, via Celoria 2, 20133 Milano, Italy.
E-mail: enrico.chiaradia@unimi.it

Key words: Vegetation; flow resistance; hydraulic roughness; riverbank stabilisation.

Acknowledgements: the research was conducted under the *Monaco Project* granted by *DG Agricoltura of Regione Lombardia (Programma regionale di ricerca in campo agricolo 2001-2003)*. We thank Ettore Fanfani, Fausto Cremascoli, Attilio Lucchini, Adolfo Rocca, and Luca, of *Consorzio Muzza Bassa Lodigiana* for their fundamental contribution to the building of the experimental channel and to the tests conduction.

Received for publication: 29 June 2018.

Accepted for publication: 8 May 2019.

©Copyright E.A. Chiaradia *et al.*, 2019

Licensee PAGEPress, Italy

Journal of Agricultural Engineering 2019; L:885

doi:10.4081/jae.2019.885

This article is distributed under the terms of the Creative Commons Attribution Noncommercial License (by-nc 4.0) which permits any non-commercial use, distribution, and reproduction in any medium, provided the original author(s) and source are credited.

or just submerged plants. Quite often, they were based on hydraulic experiments conducted in laboratory flumes, with artificial elements mimicking the real vegetation, owing to the practical difficulties involved in using real plants (Wu *et al.*, 1999; Yen, 2002; Righetti and Armanini, 2002; Stone and Shen, 2002; Wilson *et al.*, 2003; Musleh and Cruise, 2006; Yagci *et al.*, 2010; Jalonen *et al.*, 2013). When real vegetation was used, the experiments were generally conducted in small-scale laboratory flumes with young plants or tiny portions of green vegetation (Yen, 2002; Armanini *et al.*, 2005; Rhee *et al.*, 2008; Righetti, 2008; Chiaradia, 2012; Västila *et al.*, 2013). Only in very few cases have the experiments involved fully developed vegetation in real flow conditions (Yen, 2002; Freeman *et al.*, 2000; Västila *et al.*, 2013). Although small-scale experiments are fundamental to investigate the relationships between plants and flow under rigorously controlled conditions, scale issues concerning the mechanical and geometrical properties of plants as well as the hydraulic conditions can severely affect the results. In fact, the shape of shrub vegetation dynamically varies as a response to the drag force exerted by the flow. Therefore, the mutual interaction between flow conditions and vegetation is strongly related to the characteristics of plants, such as branching, foliage and stiffness (*e.g.*, Chiaradia, 2012), which are very difficult to reproduce in small-scale models. Thus, full-scale experiments are highly relevant and can provide new insights into the relationships between shrub vegetation and flow. Unfortunately, such experiments require large channels and huge volumes of water, plants and labour, and they are subject to more limitations than small-scale tests (*e.g.*, repeatability, seasonality, difficulties in measuring and controlling the hydraulic variables).

In this study, we present and discuss the results of a number of full-scale experiments conducted in a large channel equipped with real branches of riparian vegetation (*Salix* and *Alnus* spp.), considering a wide range of discharge values (up to 5 m³/s) and various plant densities, similar to those that can be observed in nature. The aim is to contribute to the knowledge of the mutual influence between shrub vegetation and flow resistance, overcoming some of the limitations affecting small-scale experiments and unnatural plant prototypes.

Materials and methods

The experimental channel

The experimental channel was obtained by adapting an existing ditch, which connects a large pumping station for land reclamation to the receiving water body (the Adda river).

Figure 1 shows a plan view of the experimental channel. A sluice gate at the channel inlet allows the control of the flow rate (Figure 1 and 2) according to the water level upstream of the gate, based on a theoretical flow-rating curve verified by actual discharge measurements. A floating gage provides continuous monitoring of the water level. The channel is 130 m long and can be split into six different reaches. The central reach (reach 4 in Figure 1) is the one in which vegetation can be placed; it is 40 m long with a bottom slope of 0.01, and it has a trapezoidal cross-section with a base width of 2 m and a side slope of 1.5 H:1 V (H=horizontal, V=vertical). The banks are lined with boulders, and the concrete bottom hosts a network of cylindrical plastic housings (0.4 m spacing) that allow the vegetation branches to be firmly anchored (Figure 2). Five stilling wells are distributed along this reach at 10 m intervals, permitting water depth measurements by floating gages. The central reach is preceded by three shorter reaches (1, 2 and 3 in Figure 1), in which the inflow from the inlet gate is smoothed to facilitate the attainment of steady state conditions at the beginning of the central reach. Finally, two terminal reaches (5 and 6 in Figure 1) gradually connect the central reach with the receiving water body. It is worth noting that through the adaptation of an existing structure, we obtained a full-scale experimental channel with a very small investment, compared with laboratory facilities of similar size. The main necessary works consisted of lining the bed of the transition and central reaches (3 and 4), creating a branch-anchoring system based on cylindrical plastic housings inserted into the concrete layer of the central reach, and installing the stilling wells along the same reach (Figure 2). However, our experimental facility suffers from some limitations compared with laboratory channels. In particular, we could not directly observe and measure the processes and variables that can

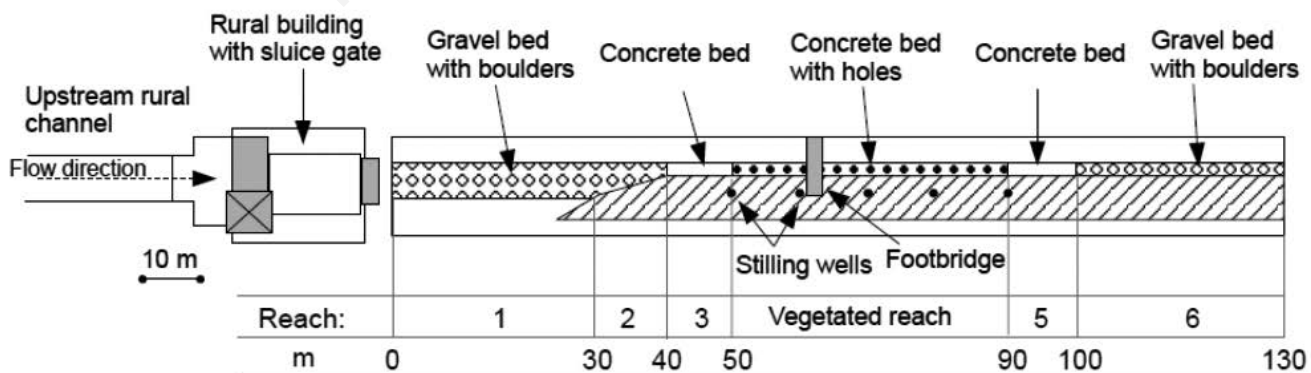


Figure 1. Plan view of the experimental channel. Water is supplied by an upstream channel and the inlet flow is controlled by a sluice gate installed in a rural building. The experimental channel consists of: two reaches (1, 2), where the inlet flow is smoothed, that are gradually linked to a transition reach (3) with the same geometry and linings of the following central reach (4) where vegetation can be placed, and two final reaches (5 and 6) linking the canal to the final receptor (a river).

be generally monitored in laboratory conditions, such as velocity profiles and plant deflection dynamics.

Experimental activity

The experimental activity that we carried out involved three riparian species: black alder (*Alnus glutinosa* L.), white willow (*Salix alba* L.) and goat willow (*Salix caprea* L.). Black alder and goat willow can be considered brush species, especially in the younger forms, that are typical of riverbanks (Eschenbach and Kappen, 1999; Dušek and Květ, 2006), since only with aging and under favourable environmental conditions they become medium and small trees, respectively (Claessens *et al.*, 2010; Dušek and Květ, 2006). White willow is a riparian tree, and we used its branches as representative of *Salix* spp in general.

For each botanical species, we considered different vegetation setups in the central reach of the experimental channel - *i.e.*, different combinations of plant species, plant density (in terms of number of plants per square meter), vegetation density and foliage status. The activity was organised in sessions, in which a fixed vegetation setup was maintained in the channel, and different experiments were carried out by changing the flow discharge.

The vegetation setups were assembled using freshly cut branches of willow and alder, randomly placed in the central reach. The mechanical and geometrical properties of the vegetation were measured shortly before the sessions. For each plant species, the sessions were carried out in sequence, from the setup with the highest vegetation density to the one with the lowest. The new setup was obtained from the previous one by removing some plants, until the desired vegetation density was reached.

During each experiment, the flow rate in the channel was kept constant - by continuously adjusting the sluice gate at the channel inlet - to guarantee stationary conditions for the time necessary to take the measurements.

Characterisation of vegetation

The mechanical properties were measured through the cantilever method (Chiaradia, 2012) described by Freeman *et al.* (2000) and applied to the entire plant. Accordingly, the modulus of

elasticity E (N/m²) was estimated as:

$$E = \frac{F \cdot b^3}{3 \cdot I \cdot \Delta} \quad (1)$$

where F is the load attached at height b (m), generating a bending of the plant stem D (m).

The stem structure was represented in a simplified form as a cylinder of diameter D_s (m), and the moment of inertia I (m⁴) was calculated as:

$$I = \frac{\pi D_s^4}{64} \quad (2)$$

Measurements of the modulus of elasticity and moment of inertia, along with plant height and diameter, were taken on thirty plants for each species before implantation in the channel bed. A summary of the measurements is reported in Table 1.

Before running each session, the stem diameter and the undeflected plant height were measured for at least thirty plants, whereas the plant density (number of stems per square meter) and the above- and below-canopy photosynthetically active radiation (PAR) values were measured at thirty or more different spots. The PAR values, representing the portion of the light spectrum that plants can use for photosynthesis, were measured using an Accupar LP 80 ceptometer (Chiaradia, 2012). The difference between complementary above- and below-canopy PAR values was used to estimate the plant area index (PAI), which represents the sum of total surface areas of all the phytoelements, *i.e.* stems and green leaves, per unit ground area (Chiaradia, 2012). We believe that PAI index is more representative of the actual vegetation biomass than the leaf area index (LAI), which considers only the foliage in case of small trees and bushes. A summary of the characteristics of the vegetation used in each session is reported in Table 2.

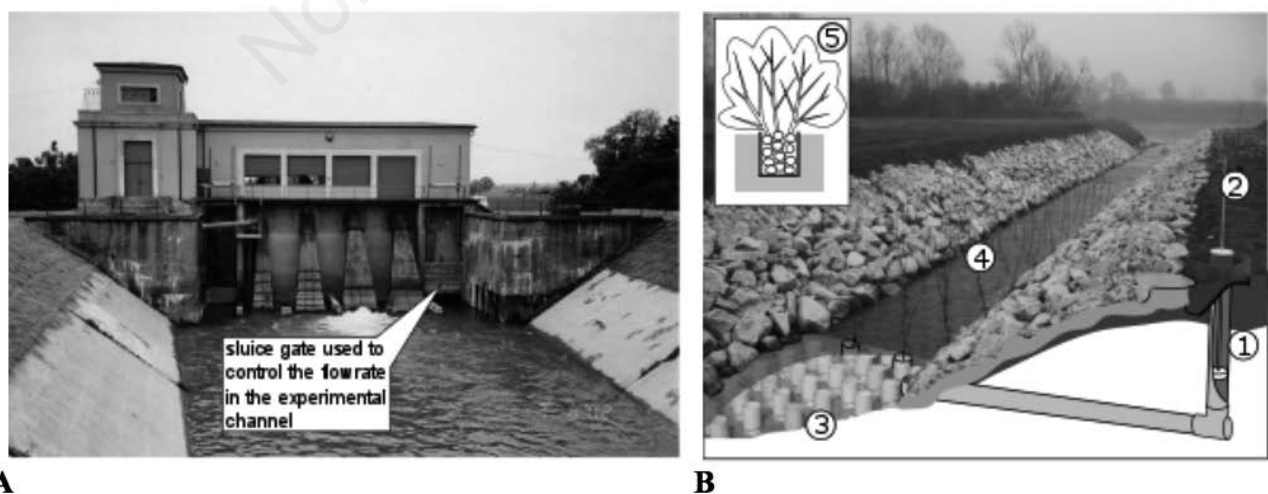


Figure 2. A view of the rural pumping station (A) and of the vegetated reach of the experimental channel (B) showing a schematic representation of the apparatus for the water depth measurement in a section (stilling well, 1, and float, 2) and of the cylindrical plastic housings inserted in the concrete bed (3) for the anchorage of the branches (4) using stones as weight (5).

Characteristics of the experimental sessions

We carried out a total of 9 sessions: 4 with white willow (*Salix alba* L.) (sessions from SA1 to SA4), 4 with goat willow (*S. caprea* L.) (sessions from SC1 to SC4), and 1 only with black alder (*A. glutinosa* L.) (session AG1) (Table 2). One additional session was conducted without any vegetation (NV session) to determine the background value of the resistance factor. The number of experiments per session ranged from a minimum of 5 (NV session) to a maximum of 10 (SA3 session), with a total of 66 experiments (Table 3).

The geometrical and mechanical characteristics of plants used in the sessions are summarised in Table 1. Stem diameter values are similar for each species (approximately 1.4 cm), whereas *A. glutinosa* differs from the others in terms of undeflected plant height, h_{veg} . The modulus of elasticity of *S. caprea* (1.9 MPa) is greater than those of *S. alba* (1.5 MPa) and *A. glutinosa*, which is the lowest (1 MPa). This finding is also reflected on the EI term (Elasticity moment of Inertia product): the willow plants showed similar EI values (4 Nm² for *S. alba* and 4.4 Nm² for *S. caprea*), whereas alder plants had the lowest value (0.7 Nm²).

The aboveground morphology was different among the species:

the alder plants consisted of a single stem with few braches in the upper half; in contrast, the willows had branched arms along the entire length of the stem and were fairly uniform in size.

The actual vegetated length of the channel varied among the sessions from 20 to 40 m, to obtain the desired experimental setting. The plant density varied from 14.8 to 2.6 stems per square meter in the SA sessions and from 17.3 to 5.4 in the SC sessions.

The PAI varied from a minimum value of 0.43 to a maximum of 1.17 (-) in the SA sessions and from 0.09 to 1.83 (-) in the SC sessions (Table 2). In the case of AG, only one vegetation density of 2.5 plants per square meter and a PAI index of 0.02 (-) were tested. Note that because PAI depends on both stems and leaves, it may significantly change for the same plant density according to the number of leaves: as an example, the PAI value of the vegetation setup of session SC2 was approximately one third of that of SC1, in spite of the fact that the two setups had the same density, with the only difference being the number of leaves.

Normally, each session was completed within 24 h, with the same branches in the channel maintained between experiments. The large dimensions of the channel and the high flow rates permitted fully turbulent flow conditions to be achieved in all experiments, dynamically and kinematically similar to those occurring in

Table 1. Plant characteristics.

Species		<i>Alnus glutinosa</i> (AG)	<i>Salix alba</i> (SA)	<i>Salix caprea</i> (SC)
Description		Young plants in pots	Just-cut branches	Just-cut branches
Plant height, h_{veg} (m)	Min	0.90	0.95	0.80
	Mean	1.70	1.47	1.52
	Max	2.20	2.20	2.40
	SD.	0.34	0.32	0.39
Plant diameter, DS (m)	Min	0.005	0.009	0.007
	Mean	0.015	0.014	0.014
	Max	0.020	0.019	0.025
	SD	0.004	0.003	0.004
Elasticity, $E \times 10^8$ (N/m ²)	Min	5.3	5.4	2.8
	Mean	10.4	15.1	19.1
	Max	19.5	29.6	48.6
	SD.	5.3	7.3	10.6
EI (Nm ²)	Min	0.31	0.18	0.12
	Mean	0.7	4.0	4.4
	Max	1.4	12.5	25.6
	SD	0.4	3.9	5.6

Table 2. Characteristics of the session.

Session	Vegetation description	Vegetated reach length (m)	Plant density (#plants/m ²)	Plant mean diameter (cm)	PAI (-)
NV	No-vegetation (reference condition)	-	-	-	-
AG1	Leafless plants	40	2.5	15.1	0.02
SA1	Leafless branches	20	14.79	13.9	0.59
SA2	Branches with few leaves at the top of stems	40	2.625	13.9	0.6
SA3	Branches with few leaves at the top of stems	20	2.625	13.9	0.43
SA4	Branches with a lot of leaves at the top of stems	20	3.75	19.9	1.17
SC1	Just-cut branches with many, uniformly distributed leaves	30	18.02	15.2	1.83
SC2	Leafless branches	30	18.02	12.4	0.55
SC3	Leafless branches	40	11.7	11.9	0.34
SC4	Leafless branches	40	5.4	10.9	0.09

natural rivers (e.g., Babaeyan-Koopaei *et al.*, 2002; Västila *et al.*, 2013) and similar to those experimented by Freeman *et al.* (2000). In fact, the Reynolds number ($Re=VR/\nu$; Yen, 2002) and velocity values were in the range of 0.2-1.0 10^6 (-) and 0.6-2.4 m/s, respectively (Table 3).

Estimation of the resistance due to vegetation

Isolating the effect of vegetation from the total resistance of the vegetated reach is not straightforward. The simplest and most widely used approach consists of splitting up the total resistance into different additive components (e.g., Freeman *et al.*, 2000; Yen, 2002; Sellin *et al.*, 2003; Green, 2005; Rhee *et al.*, 2008; Jalonen *et al.*, 2013; Västilä *et al.*, 2013). In our case, two components are relevant: the resistance of the non-vegetated wetted perimeter, expressed by the roughness coefficient n_b , and the additional contribution of the vegetation, expressed by the roughness coefficient n_{veg} . Therefore, we assumed that the total roughness coefficient n is given by:

$$n = n_b + n_{veg} \tag{3}$$

Both n_b and n_{veg} are expected to change with varying water level in the channel, given the heterogeneity of the channel section and the dynamic behaviour of flexible vegetation. Therefore, we used the observations collected in each of the five experiments with no vegetation and in each of the 61 experiments with vegetation, described in the previous section, to derive as many values of n_b and n_{veg} as possible. In fact, for each experiment, the measurements of Q and the water elevation y_i at the control sections in steady-state conditions were available, similar to other studies on just submerged vegetation (e.g., Rhee *et al.*, 2008; Righetti, 2008; Västilä *et al.*, 2013). This allowed us to estimate the unknown value of the total Manning coefficient n through an iterative procedure that minimises the root mean square error (RMSE) between the measured water elevations and the values obtained at the same sections by the numerical integration of the energy equation between the initial and final sections of the central reach.

The discrete form of the energy equation for two consecutive sections, i and $i+1$, is:

$$\frac{H_{i+1} - H_i}{(x_{i+1} - x_i)} = -\frac{(S_{fi} - S_{fi+1})}{2} \tag{4}$$

where H_i (m) is the energy level at section i , S_{fi} (-) is the slope of the energy line at the same section, and x_i is the coordinate of the section along the channel. Standard step method (SSM) was applied with 1 m spacing between sections. The channel geometry was derived from direct survey at a number of sections (approximately every 5 m) and from linear interpolation for intermediate sections.

The energy level in section i is given by:

$$H_i = z_i + h_i + \alpha \frac{V_i^2}{2g} = y_i + \alpha \frac{V_i^2}{2g} \tag{5}$$

where z_i is the bed elevation (m); h_i is the flow depth (m); α is the Coriolis coefficient, which is assumed to be 1 because of the fully turbulent regime of the flow in the channel; g (m/s^2) is the gravitational acceleration constant; V_i (m/s) is the mean flow velocity; and y_i is the water elevation in the channel (m).

The friction slope is given by:

$$S_f = \left(\frac{nQ}{AR^{2/3}} \right)^2 \tag{6}$$

where n ($m^{1/3}/s$) is the Manning coefficient, Q (m^3/s) is the discharge, A (m^2) is the wetted area of the section, and R (m) is the hydraulic radius.

At each step of the estimation procedure, the energy profile corresponding to the current value of n is computed using the SSM (Subhash, 2001) to solve the integration problem, and the RMSE value of the observed vs. simulated water levels is then computed. The procedure terminates when the variation of the value of n between two subsequent steps is less than 0.001, which corresponds to an accuracy in the discharge estimation >97%, which can be considered acceptable for practical use and consistent with the experimental setup.

The five values of the Manning coefficient of the non-vegetated wetted perimeter obtained from the experiments of the NV session were then related to the corresponding average water level in the experimental reach, \bar{h} , to obtain the $n_b(\bar{h})$ relationship to be used with Equation (3) to derive the n_{veg} values for the experiments with vegetation. Because the section is non-homogenous, with higher roughness of the boulder banks than that of the concrete

Table 3. Hydraulic characteristics of each experimental session (n_{eq} = total Manning's roughness coefficient, Re = Reynold's number).

Session	Number of experiments	Flow rate (m^3/s)		Water level (m)		Velocity (m/s)		n_{eq} ($m^{-1/3}s$)		Re (-)	
		Min	Max	Min	Max	Min	Max	Min	Max	Min	Max
NV	5	1.0	5.0	0.24	0.63	1.69	2.68	0.022	0.025	$340 \cdot 10^3$	$1139 \cdot 10^3$
AG1	6	0.5	3.0	0.18	0.51	1.22	2.08	0.025	0.031	$183 \cdot 10^3$	$763 \cdot 10^3$
SA1	7	1.0	3.0	0.48	0.86	0.78	1.09	0.070	0.092	$275 \cdot 10^3$	$562 \cdot 10^3$
SA2	7	0.75	4.45	0.34	0.83	0.85	1.62	0.049	0.062	$227 \cdot 10^3$	$829 \cdot 10^3$
SA3	10	0.50	5.0	0.25	0.88	0.79	1.66	0.049	0.065	$165 \cdot 10^3$	$887 \cdot 10^3$
SA4	8	0.50	5.0	0.22	0.85	0.97	1.80	0.032	0.060	$174 \cdot 10^3$	$955 \cdot 10^3$
SC1	8	0.50	5.0	0.35	0.99	0.56	1.47	0.061	0.093	$155 \cdot 10^3$	$840 \cdot 10^3$
SC2	8	0.50	5.0	0.31	0.91	0.65	1.66	0.051	0.080	$162 \cdot 10^3$	$901 \cdot 10^3$
SC3	8	0.50	5.0	0.26	0.82	0.77	1.84	0.042	0.055	$163 \cdot 10^3$	$934 \cdot 10^3$
SC4	8	0.50	5.0	0.18	0.89	1.16	2.37	0.027	0.041	$181 \cdot 10^3$	$1063 \cdot 10^3$

bottom, the relationship is expected to be nonlinear, according to the most widely recognised methods to estimate the total roughness of composite sections (e.g., Yen, 2002). Therefore, we used a power function to interpolate the roughness vs. water level rating curve, obtaining

$$n_b = 0.027 \bar{h}^{0.142} \quad (R^2=0.90) \quad (7)$$

where \bar{h} is the average water depth.

Almost the same relationship is obtained by applying the Einstein-Horton method with roughness coefficient values that are consistent with the section characteristics ($0.31 \text{ m}^{-1/3}\text{s}$ and $0.21 \text{ m}^{-1/3}\text{s}$ for the banks and bottom, respectively, based on Chow, 1959).

Results

The results are presented in terms of Manning's coefficient as a function of the product VR (m^2/s), proportional to the Reynolds

number, the ratio h/h_{veg} (-) between water depth and undeflected vegetation height and the plant Reynolds number introduced by Armanini *et al.* (2005) and Righetti (2008):

$$Re_p = VD_s/\nu \quad (8)$$

where D_s is the average stem diameter, and ν is the kinematic viscosity.

Alnus glutinosa session

The results of the 6 *Alnus glutinosa* (AG) experiments are shown in Figure 3. It can be noted that the presence of low-density leafless plants characterised by a single stem and few branches in the upper half did not greatly impact the hydraulic resistance. The range of the additional Manning coefficient, n_{veg} (obtained from Eq. 8), is within the range specified by Arcement and Schneider (1987) as small and typical of a tree seedling growing where the average flow depth is three times the height of the vegetation.

Although the variation of n_{veg} with hydraulic conditions is

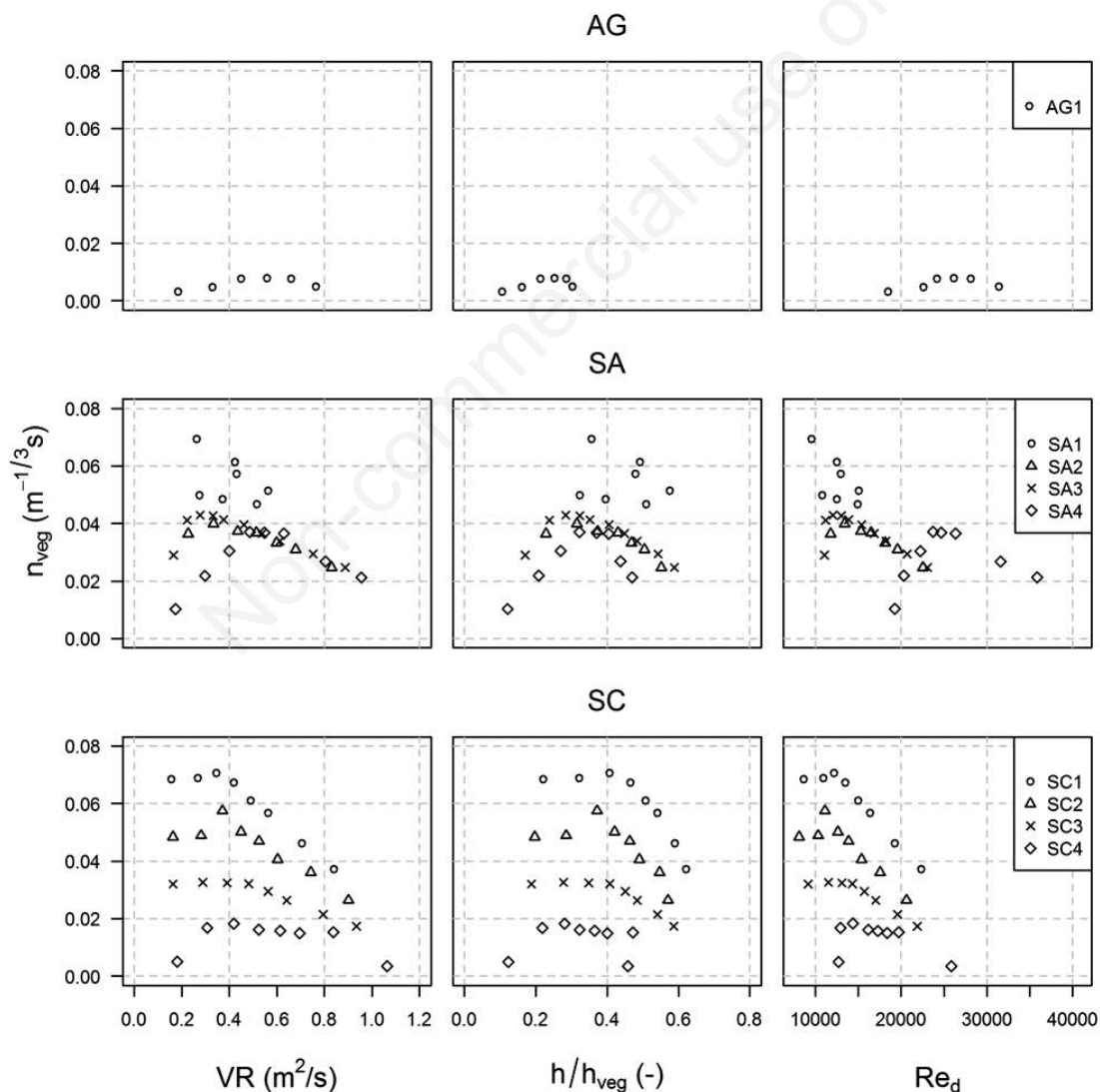


Figure 3. Estimated n_{veg} -values against VR product, h/h_{veg} and Red for black alder (*Alnus glutinosa*, AG), white willow (*Salix alba*, SA) and goat willow (*Salix caprea*, SC).

small, it showed a moderately rising trend with VR , h/h_{veg} and Re_p followed by a falling limb. The maximum n_{veg} of $0.008 \text{ m}^{-1/3}\text{s}$ was observed at a VR value of $0.56 \text{ m}^2/\text{s}$, corresponding to a ratio between the water level and the undeflected plant height, h/h_{veg} , of 25%, and an Re_p value of 26.2×10^3 .

The minimum values of n_{veg} occurred at the lowest value of VR , h/h_{veg} and Re_p ($n=0.004 \text{ m}^{1/3}\text{s}$ at $VR = 0.18 \text{ m}^2/\text{s}$, $h/h_{veg} = 10\%$, and $Re_d = 18.5 \cdot 10^3$).

The undeflected submergence ratio is generally low, less than 0.4 for all flow conditions, which can be related to the geometry of plants (single stem) and to the tested density. Plants, in fact, did not significantly bend until VR exceeded the value of 0.4; afterwards, the plants bent, and the deflected height became similar to the flow depth. At higher VR values, the submergence ratio increased, but it could not be measured owing to the limitations of our experimental channel, in which we could not systematically observe the bent plant height and then evaluate with sufficient accuracy the changes of the vegetated layer thickness, as for example in Righetti (2008).

Salix alba sessions

The effect of white willow branches on the hydraulic resistance was always relevant but variable according to plant density and PAI.

The most flow-obstruent vegetation setup was the one used in session *Salix alba* (SA) 1 (which is the densest, although the PAI values were smaller than those in the other SA sessions; Table 2), with the estimated values of n_{veg} ranging between 0.044 and $0.067 \text{ m}^{-1/3}\text{s}$. The range of n_{veg} is in agreement with Arcement and Schneider (1987), which would classify it as a very large effect, typical of moderate to dense brush.

The vegetation setups of sessions SA2 and SA3, which are rather similar except for PAI values (Table 2), resulted in similar ranges of n_{veg} values, between 0.023 and $0.041 \text{ m}^{-1/3}\text{s}$. The obstruent effect of such configurations can be considered large and, according to Arcement and Schneider (1987), typical of 8- to 10-year-old willow or cottonwood trees intergrown with some weeds and brush (none of the vegetation in foliage).

The vegetation setups of session SA4, which is denser than that of SA2 and SA3 and has a higher PAI value, resulted in a less obstruent effect with n_{veg} values ranging between 0.011 and $0.035 \text{ m}^{-1/3}\text{s}$. The obstruent effect is classified as medium and typical of brushy, moderately dense vegetation, similar to 1- to 2-year-old willow trees in the dormant season (Arcement and Schneider, 1987).

In general, configurations with smaller plant density values induced similar resistance, regardless of the presence of leaves (Figure 3). SA4, in spite of a slightly higher density than that of SA2 and SA3, showed a minor effect at low values of VR , h/h_{veg} , and Re_p , perhaps because the shrub used in SA4 was different from those used in the other experiments and possibly had a slightly different branching structure.

The results of all the sessions, except SA1 (the most flow-obstruent), showed a two-stage trend in the n_{veg} vs. VR and h/h_{veg} and Re_p relationships, with the position of the threshold point changing from one session to the next. This corresponds to a VR value of approximately $0.3 \text{ m}^2/\text{s}$ for SA2 and SA3 and $0.5 \text{ m}^2/\text{s}$ for SA4, h/h_{veg} of approximately 30% of the plant height in all experiments and a Re_p value of approximately $12 \cdot 10^3$ for SA2 and SA3 and $25 \cdot 10^3$ for SA4. It must be underlined that the threshold values are similar for most configurations, except for SA4 and for SA1 (where only the decreasing trend was detected). Moreover, all the n_{veg} vs. VR patterns tend to converge towards the same value of n_{veg} as VR increases.

Finally, it is evident that for SA4 the trend of n_{veg} values with Re_p is different from the others as a consequence of a different branch diameter distribution (Table 2).

Salix caprea sessions

The results of the 32 experiments of the four *Salix caprea* (SC) sessions are shown in Figure 3. In general, n_{veg} values decrease passing from SC1 (0.035 to $0.068 \text{ m}^{-1/3}\text{s}$) to SC2 (0.025 to $0.055 \text{ m}^{-1/3}\text{s}$), SC3 (0.016 – $0.032 \text{ m}^{-1/3}\text{s}$) and SC4 (0.003 to $0.017 \text{ m}^{-1/3}\text{s}$), according to plant density and PAI values. SC1, the vegetation setup with the highest density and PAI values, could be classified as having a large to very large effect, SC2 as large, SC3 as medium to large, and SC4 as small to medium (Arcement and Schneider, 1987).

The sessions show a variously marked two-stage trend, with the maximum n_{veg} value at which the reversal occurs, at values of VR of approximately $0.40 \text{ m}^2/\text{s}$, h/h_{veg} of 30–40% (41% for SC1, 37% for SC2, 41% for SC3 and 28% for SC4) and Re_p of $14 \cdot 10^3$. The falling phase is more pronounced in SC1, SC2 and SC3, whereas in SC4 a central flat portion can be observed. The n_{veg} vs. VR trends converge to a unique value of n_{veg} as VR increases, as in the case of the SA sessions.

Comparing the SC1 and SC2 sessions, which have similar values of plant density and a small difference in PAI values (owing to the leaf presence in SC2), it can be noticed that the additional roughness component due to the presence of leaves is approximately $0.015 \text{ m}^{-1/3}\text{s}$; the same value is obtained with a halved density when the branches are leafless (compare SC2, SC3 and SC4).

Discussion

The values of the additional Manning's coefficient obtained in our experimental sessions span over a wide range, depending mainly on plant species, density and partially foliage condition. The observed ranges of variability are consistent both with results from previous studies (e.g., Cowan, 1956; Chow, 1959; Bakry *et al.*, 1992) and with the values suggested by technical literature (Arcement and Schneider, 1987). Within the same session, Manning's coefficient varied significantly for different flow conditions, proving that a constant, flow-independent value of the roughness coefficient is not adequate to describe the real behaviour of riparian vegetation, in contrast to what is frequently carried out in practical applications (e.g., Chow 1959). This confirms the results of small-scale laboratory experiments (Yen, 2002; Armanini *et al.*, 2005; Rhee *et al.*, 2008; Righetti, 2008), which, however, highlight only a part of the whole phenomenon. One of the main results of our full-scale experiments, in agreement with Freeman *et al.* (2000), is the evidence of a changing behaviour of partially flexible and partially submerged vegetation (Figure 3). This is particularly clear in the SC series, in which the implementation of the experiments benefitted from experience gained during the previous AG and SA sessions.

The results show that in all sessions except one (SA1), there is two-stage trend in the values of the additional hydraulic resistance at changing flow conditions, with the same vegetation setup. Initially, the hydraulic resistance increases with VR , h/h_{veg} and Re_p , as in the case of unsubmerged rigid bodies; then, after reaching a maximum, the resistance decreases with VR , h/h_{veg} and Re_p , as in the case of submerged flexible bodies.

Actually, at low flows, which are characterised by small water depth and velocity values, the vegetation is only partially sub-

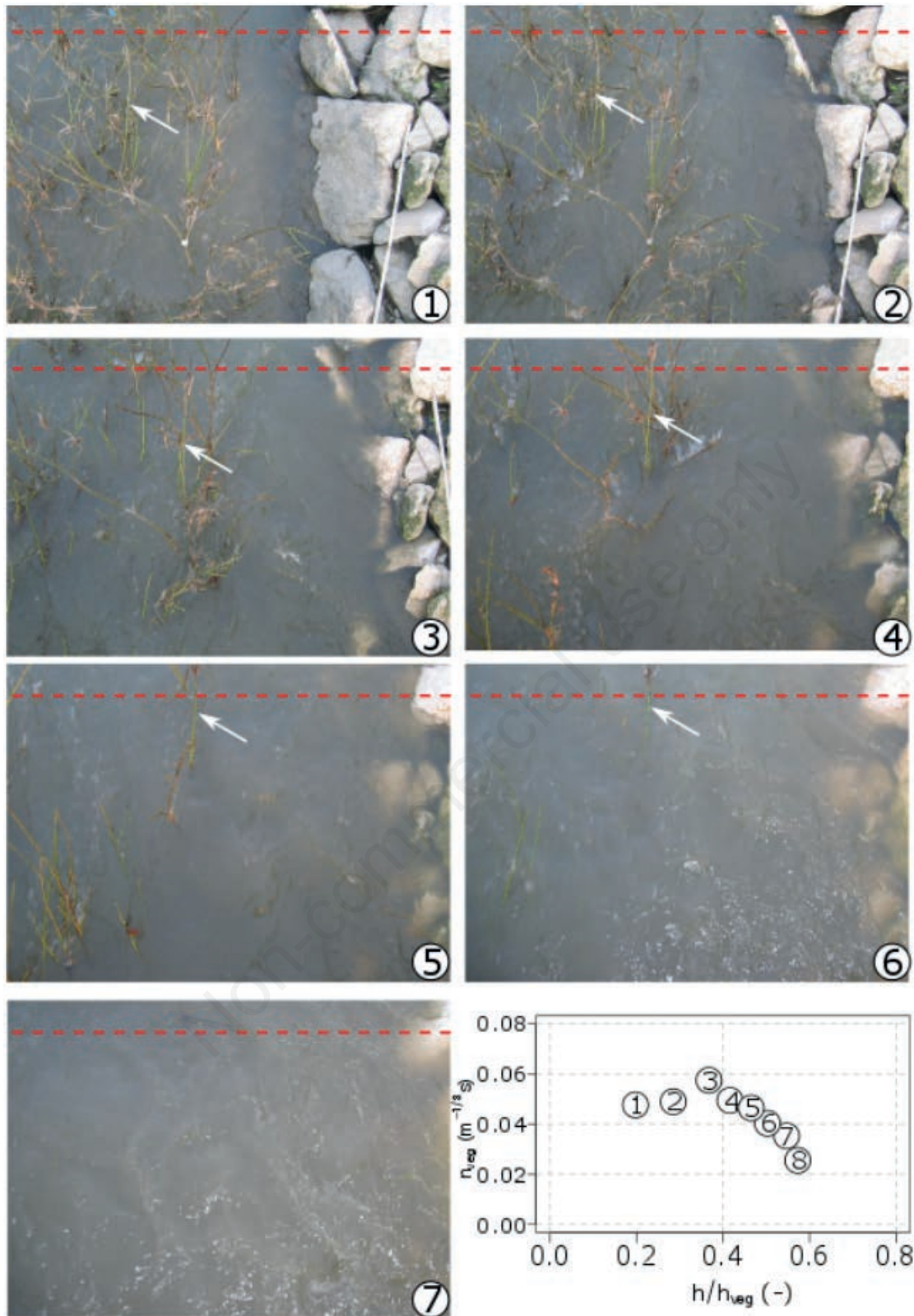


Figure 4. Plant bending with the increasing of the submersion. Numbers refer to the value of Manning coefficients in the chart at the bottom (*i.e.* SC2 series). Note that only part of the vegetation was submerged when the maximum roughness value is obtained (picture and point 3). With the lowest discharge, the vegetation was weakly bended and it was stable (1); at higher discharge, stems were downstream orientated (2); then, vibration of stiff vertical stems and a sinuous movement of oblique or elongated horizontal stems occurred (3); stiff stems become more inclined (4); stems become prone or densely compacted (5); at the highest discharges, plants were completely submerged and bended at the bottom (6, 7 and 8). Use the red line as position reference.

merged and the water flow impacts only on the stem and on the main branches, due to the typical distribution of branches and leaves along the height of riparian shrubs. Because the stem and the main branches are rather stiff, the resulting resistance behaves as in the case of rigid bodies. However, at higher flows both water height and water velocity increase and so does the force impacting on stems, main and minor branches and leaves; when it reaches a value that is sufficient to bend them, the plant tends to assume a more streamlined shape (Figure 4). The point at which these effects clearly emerge, marked as *threshold point* in the n - VR , n - h/h_{veg} and n - Re_p diagrams, is not fixed, although it varies in a rather small range, between approximately 0.3 and 0.5 m^2/s for VR and 30-40% for h/h_{veg} . Freeman *et al.* (2000) reported a fixed position of the threshold point at h/h_{veg} of 80%, based on the observation that, during the experiments, plants bent at this level of submergence. We believe that this difference in the threshold point position can be ascribed to the higher velocity values in our experiments, since the other conditions are similar in the two studies: the stiffness of the plants falls in the same range, the flow depth values are close and the hydraulic conditions sub-critical. It must be noted that in the SA1 session, where the vegetation setup consists of highly flexible branches, the two-stage trend of n_{veg} did not emerge. This result occurs because the hydrodynamic force was sufficient to bend the branches already in the experiment with the smallest flow rate; therefore, only the second phase of the pattern could be observed, with the n_{veg} values decreasing with increasing flow rate (Figure 4). As a consequence of such dynamics, the additional resistance due to plants deviates from the velocity-squared relationship typical of rigid bodies and decreases with velocity (Yen, 2002; Västilä *et al.*, 2013).

The evidence of a two-stage trend of the of the n vs. velocity or submergence ratio relationship that emerges from our experiments is in agreement with the results of Freeman *et al.* (2000) and, to some extent, of Rhee *et al.* (2008), whereas other works on partially flexible vegetation observed only a reduction of resistance with velocity and/or submergence ratio (Västilä *et al.*, 2013). This can be due to the differences in the scale of the experimental, the level of submergence and the branching structure of the vegetation used in the various studies. Our results, as well as those of Freeman *et al.* (2000), refer to full-size branches (1.0-2.0 m in height and 1-2 cm in diameter), under fully turbulent flow conditions, that are similar to those of real watercourses.

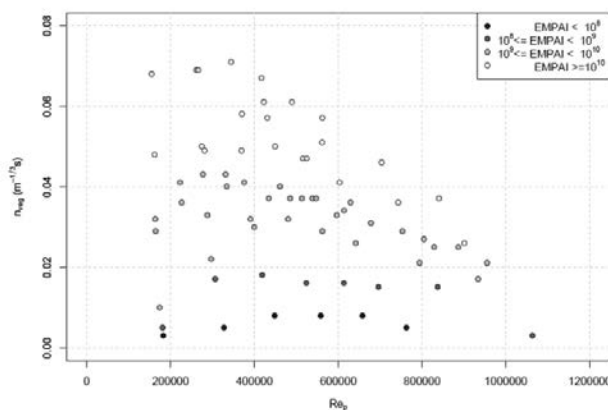


Figure 5. Values of n_{veg} at changing Re_p ; points are grouped in four classes of $E \cdot M \cdot PAI$ values.

Armanini *et al.* (2005) and Righetti (2008) suggested consideration of a modified submergence ratio in which the bent plant height is taken instead of the full plant height. In our case, for practical reasons, it was impossible to measure such a deflected height; in any case, we deem that considering h/h_{veg} is better for practical applications (h_{veg} can be easily measured or estimated) and for comparison with most of the results already available in the literature.

The role of plant density emerged clearly, but it is not the single factor that determines the additional resistance due to riparian vegetation. Comparing the same species in the same leafless condition, but with a different plant density (also reflected by PAI values), as for SA1, SA2 and SA3 and SC2 and SC3, this role is evident (Figure 3 and Table 2). The difference in n_{veg} is approximately 0.03 $m^{1/3}s^{-1}$ for SA and 0.015 $m^{1/3}s^{-1}$ for SC passing from 14.8 to 2.6 plants/ m^2 and from 18.0 to 11.7 plants/ m^2 , respectively.

The number of plants per unit area, however, is insufficient to characterise the vegetation. To consider plant characteristics, the friction factor was successfully normalised by LAI for the case of the foliated single-stem portion of plants (Västilä *et al.*, 2013). In the case of multi-branch riparian vegetation, however, the process is more complex and LAI is unable alone to fully explain the roughness dynamics (Freeman *et al.*, 2000). We then combined plant density (M), PAI and the modulus of elasticity (E), to account for the main factors affecting the additional resistance due to riparian vegetation. In Figure 5, the results of the experiments are grouped by the values of the product of the abovementioned variables ($E \cdot M \cdot PAI$). It can be noted how n_{veg} values increase with increasing combined index, and values with the combined index within the same order of magnitude can be grouped together.

Considering all our results (Figure 5), it can be noted that the values of additional n_{veg} tend toward a unique value as Re increases. This can be explained considering the characteristic of tested plants: branches bend and shrink as hydrodynamic forces impact them until a structural limit, related to the stiffness characteristics and topology of branches, is reached (Yen, 2002; Freeman *et al.*, 2000; Armanini *et al.*, 2005).

The role of leaves on the total resistance is significant and decreases with increasing VR as a consequence of streamlining, as recently demonstrated by Västilä *et al.* (2013). At the same time, however, the experiments carried out with leafless plants demonstrate that the bending of the stem and the main braches is also fundamental within the dynamics of plants resistance. By comparing SC1 and SC2, in which the main difference is the presence of leaves in the latter, the difference in maximum n_{veg} is <20%, whereas Västilä *et al.* (2013) estimated a difference between 60% and 70%. In our case, however, plants are full-scale multiple branched shrubs, and the role of branch stiffness is greater than that in the small-scale single-stem plants used by Västilä *et al.* (2013). The topological structure and stiffness characteristics of plants, as a consequence, play a fundamental role in the flow-plant mutual interaction. Remarkably, in many climatic regions, riparian vegetation is deciduous and floods occur when plants are leafless, so that the additional resistance due to branches very likely exceeds the effect of leaves (Figure 4).

Conclusions

In this paper, we presented the results of full-scale experiments aimed to evaluate the hydraulic resistance due to partially flexible riparian vegetation, conducted under different hydraulic conditions and different plant configurations (species, density and leaf presence).

The results show that riparian vegetation behaves differently under different hydraulic conditions as a consequence of changing plant-flow interaction. Riparian plants behave as a rigid body when VR and/or h/h_{veg} and/or Re_p values are limited; consequently, resistance to flow increases. When a threshold value of VR and/or h/h_{veg} and/or Re_p is reached, the resistance decreases as a result of stem and branch bending and/or leaf-branch compaction; this process proceeds with increasing VR and/or h/h_{veg} and/or Re_p . This two-stage trend is in agreement with Freeman *et al.* (2000) and partially with Rhee *et al.* (2008) and is not captured by small-scale experiments. The threshold point in resistance values varies in a rather small range for significantly different plant densities and conditions (level of foliage) and seems to be related to the combined effect of stiffness, submergence ratio and flow velocity.

The plant characteristics (number, position and size of branches on the main stem) and the plant density seem to play a relevant role. In fact, when poorly branched plants at low densities are considered, resistance coefficient is small and differences between different hydraulic conditions are small too, since leaves and flexible minor branches already take an increasingly streamlined shape for small values of velocity (*e.g.*, Västilä *et al.*, 2013) and the effect of plants on the hydraulic resistance is nearly constant. On the contrary, when high-density vegetation conditions are analysed, the Manning's coefficient varies considerably at changing hydraulic conditions and the two-stage trend is well recognisable.

According to Västilä *et al.* (2013), foliage is a significant source of hydraulic resistance; from our experiments, this effect can be estimated on the order of $0.015 \text{ m}^{-1/3}\text{s}$. Plant density, however, can be of great importance as well. In our experiments, when leafless plant densities were doubled, an increase of Manning's n value on the order of $0.02 \text{ m}^{-1/3}\text{s}$ was estimated.

We believe that these findings, which are based on full-scale experiments in terms of both plant size and flow characteristics, may contribute to improving the understanding of the interactions between flow and riparian vegetation; this understanding is fundamental for the design of riverbank soil bioengineering and stream restoration works and, more generally, for naturally oriented management of surface water bodies.

References

- Arcement G.J., Schneider V.G. 1987. Roughness coefficients for densely vegetated floodplains. *Water Res Investig Rep* 83-4247, USGS, 34 pp.
- Babaeyan-Koopaei, K, Ervine D.A, Carling. P.A., Cao Z. 2002. Velocity and Turbulence Measurements for Two Overbank Flow Events in River Severn, *J. Hydraul. Eng.* 128:891-900.
- Bakry M.F., Gates T.K., Khattab A.F. 1992. Field-measurement hydraulic resistance characteristics in vegetation-infested canals. *J. Irr. Drain. Eng.* ASCE 118;2.
- Bal K., Struyf E., Vereecken H., Viaene P., De Doncker L., de Deckere E., Mostaert F., Meire P. 2011. How do macrophyte distribution patterns affect hydraulic resistances? *Ecol. Eng.* 37. 529-33.
- Bennett S.J., Simon A. 2004. Riparian vegetation and fluvial geomorphology. American Geophysical Union, Washington, DC, USA.
- Bebina Devi T., Kumar B. 2016. Flow characteristics in an alluvial channel covered partially with submerged vegetation. *Ecol. Eng.* 94:478-92.
- Carollo F., Ferro V., Termini D. 2005. Flow resistance law in channels with flexible submerged vegetation. *J. Hydr. Eng. ASCE* 131:554-64.
- Chiaradia E.A. 2012. L'uso del plant area index per la determinazione del coefficiente di scabrezza della vegetazione arbustiva. In: XXXIII Convegno Nazionale di Idraulica e Costruzioni Idrauliche, Brescia, Italy.
- Chow V.T. 1959. Open channel hydraulics. McGraw-Hill, New York, NY, USA.
- Claessens H., Oosterbaan A., Savill P., Rondeux J. 2010. A review of the characteristics of black alder (*Alnus glutinosa* (L.) Gaertn.) and their implications for silvicultural practices. *Forestry* 83:163-75.
- Dušek J., Květ J. 2006. Seasonal dynamics of dry weight, growth rate and root/shoot ratio in different aged seedlings of *Salix caprea*. *Biologia*. 61:441-7.
- Errico A., Pasquino V., Maxwald M., Chirico G.B., Solari L., Preti F. 2018. The effect of flexible vegetation on flow in drainage channels: estimation of roughness coefficients at the real scale. *Ecol. Eng.* 120:411-21.
- Eschenbach C., Kappen L. 1999. Leaf water relations of black alder [*Alnus glutinosa* (L.) Gaertn.] growing at neighbouring sites with different water regimes. *Trees* 14:28-38.
- FISRWG. 1998. Stream corridor restoration: principles, processes, and practices. by the Federal Interagency Stream Restoration Working Group. (FISRWG) (15 Federal agencies of the US gov't). GPO Item No. 0120-A; SuDocs No. A 57.6/2:EN 3/PT.653.
- Freeman G.E., Rahmeyer W.H., Copeland R.R. 2000. Determination of resistance due to shrubs and woody vegetation. Final report US Army Corps of Eng, Washington, DC, USA.
- Green J. 2005. Comparison of blockage factors in modelling the resistance of channels containing submerged macrophytes. *River Res. Appl.* 21:671-86.
- Järvelä J. 2004. Determination of flow resistance caused by non-submerged woody vegetation. *Int. J. River Basin Manag.* 2:61-70.
- Kirkby J.T., Durras S.R., Pitt R., Johnson D. 2005. Hydraulic resistance in grass swales design for small flow conveyance. *J. Hydr. Eng. ASCE* 131:65-8.
- Kothyari U.C., Hayashi K., Hashimoto H. 2009. Drag coefficient of unsubmerged rigid vegetation stems in open channel flows. *J. Hydraul. Res.* 47:691-9.
- Li Y., Wang Y., Ofosu Anim D., Tang C., Du W., Ni L., Yu Z., Acharya K. 2014. Flow characteristics in different densities of submerged flexible vegetation from an open-channel flume study of artificial plants. *Geomorphology* 204:314-24.
- Merritt D.M., Scott M.L., Poff N.L., Auble G.T., Lytle D.A. 2010. Theory, methods and tools for determining environmental flows for riparian vegetation: riparian vegetation-flow response guilds. *Freshwater Biol.* 55:206-25.
- Ming R.H., Shen H.W. 1973. Effect of tall vegetation on flow and sediment. *J. Hydr. Div. ASCE* 99:793-814.
- Musleh F.A., Cruise J.F. 2006. Functional relationship in wide flood plains with rigid unsubmerged vegetation. *J. Hydr. Eng. ASCE* 132:163-71.
- Nepf H.M. 2012. Hydrodynamics of vegetated channels. *J. Hydr. Res.* 50:262-79.
- Pusey B.J., Arthington A.H. 2003. Importance of the riparian zone to the conservation and management of freshwater fish: a review. *Marine Freshwater Res.* 54:1-16.
- Rhee D.S., Woo H., Kwon B.A., Ahn H.K. 2008. Hydraulics resistance of some selected vegetation in open channel flows. *River Res. Appl.*, 24: 673-87.
- Righetti M. 2008. Flow analysis in a channel with flexible vegetation using double-averaging method. *Acta Geophys.* 56:801-23.

- Righetti M., Armanini A. 2002. Flow resistance in open channel flow with sparsely distributed bushes. *J. Hydrol.* 269:55-64.
- Sellin R.H.J., Bryant T.B., Loveless J.H. 2003. An improved method for roughening floodplains on physical river models. *J. Hydr. Res.* 41:3-14.
- Stone B.M., Shen H.T. 2002. Hydraulic resistance of flow in channels with cylindrical roughness. *J. Hydr. Eng. ASCE* 128:500-6.
- Subhash C.J. 2001. *Open-channel flow*. John Wiley and Sons ed., New York, NY, USA, 328 pp.
- Temple D.M. 1999. Flow resistance of grass-lined channel banks. *Appl. Eng. Agric.* 15:129-33.
- Västilä K., Järvelä J., Aberle J. 2013. Characteristics reference area for estimating flow resistance of natural foliated vegetation. *J. Hydrology* 492:49-60.
- Wilson C.A.M.E., Stoesser T., Bates P.D., Batemann Pinzen A. 2003. Open channel flow through different forms of submerged flexible vegetation. *J. Hydraul. Eng.* 129:847-53.
- Wu F.-C., Shen H.W., Chou Y.-J. 1999. Variation of roughness coefficient for unsubmerged and submerged vegetation. *J. Hydr. Eng. ASCE* 125:934-42.
- Yagci O., Tschiesche U., Kabdasi M.S. 2010. The role of different forms of natural riparian vegetation on turbulence and kinetic energy characteristics. *Adv. Water Resour.* 33:601-14.
- Yen B.C. 2002. Open channel flow resistance. *Hydr. Eng. ASCE* 128:20-39.

Non-commercial use only